

Fight Control of Flying Test Bed for Future Planetary Landing

By Takehiro HIGUCHI,¹⁾ Toshiki TAMURA,¹⁾ Seiya UENO,¹⁾ Kazuhisa FUJITA,²⁾ Takashi OZAWA,²⁾ and Hiroki TAKAYANAGI²⁾

¹⁾Yokohama National University, Yokohama, Japan

²⁾Chofu Aerospace Center, JAXA, Tokyo, Japan

(Received April 24th, 2017)

This paper is on flight control of Flying Test Bed (FTB) for future planetary landing. The FTB is a test bed to be used on the earth to demonstrate the ability of guidance, navigation and control systems. The FTB has unique ability where it has enough force to lift in gravitational environment of the earth but very low specific impulse. This will lead to the problem where the thrust has strong delay for firing as well as shutdown. This delay and low specific impulse leads to difficulty of designing the robust guidance and control for the system. The paper introduces these difficulties and shows the result of the robust control law for the FTB. The control law is examined through the simulations with thrust / thrust angle errors and shown the robustness against possible errors that appears in the actual flight.

Key Words: Flying Test Bed, Planetary Landing, Soft Landing, Time Delay

Nomenclature

m	: mass
I	: moment of inertia
T	: Thrust
X, Y, Z	: position
u, v, w	: velocity
θ, ϕ, ψ	: attitude angle (Euler angle)
ω	: angular velocity
g_E	: gravitational constant
I_{sp}	: specific impulse
$Arm1$: length to the further thruster from center
$Arm2$: length to the closer thruster from center
t	: time
U	: input force for each thruster
ζ, ω	: gain for control law

Subscripts

D	: dry condition
x, y, z	: direction / rotational axis
M	: main thruster
R	: roll (sub) thruster
r	: reference

1. Introduction

The Flying Test Bed for future planetary landing aims to test the navigation, guidance and control law for future planetary landing. Recently, the planetary landing has been popular throughout the world targeting on moon, the Mars and beyond. Japan is now planning some planetary landing missions starting from the SLIM project in FY2019¹⁾. Although there are some projects and researches that are

proceeding, Japan does not have a FTB that could be used to check the navigation, guidance and control system for the landing, whereas USA has developed various flying test beds such as Morpheus²⁾, Mighty Eagle³⁾ and Xombie⁴⁾. In Japan, there used to be a FTB projects^{5,6)} aiming for the SELENE projects, but they did not last as a permanent test bed to be used for planetary landing.

JAXA has begun the development of the planetary landing FTB to experiment future planetary landing^{7,8)}. Figure 1 is the image of the FTB by JAXA. The FTB has eight 200N class main thrusters and four 2N class yaw thrusters for altitude and attitude control. One of the difficulties for the control system for the FTB is the time delay that appears for activating and terminating the main thrusters. From the ground test, 40ms of activation delay and 80ms of termination delay has been measured. The time delay does appear in various control systems but the problem is critical for the FTB system where the gravity force is basically larger than the target planets, the main thrusters have to control the roll/pitch attitude and the altitude at the same time, the center of gravity of the system is

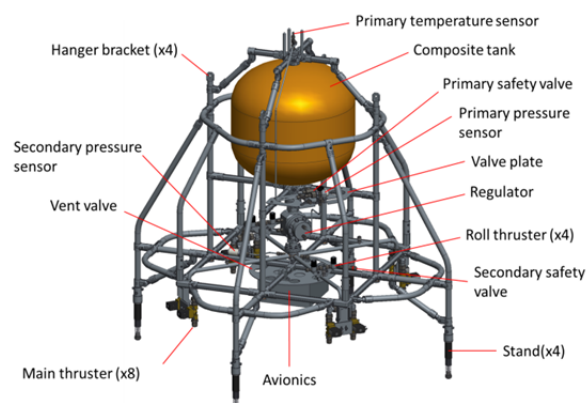


Fig.1 Setup of Flying Test Bed.

Table 1 Specifications of the Flying Test Bed.

Item	Specification	
Mass (m) [kg]	Dry	78.5
	Wet	95.0
Center of gravity(x, y, z) [m] (Dry)	(0.0061, 0.0043, 0.2034)	
Moment of Inertia [kg·m ²] (Dry)	I_{Dxx}	19.522
	I_{Dyy}	19.491
	I_{Dzz}	12.066
Main thruster (T_M) [N]	173.5±3.5	
Specific impulse (I_{spM}) [s]	49.6	
Roll thruster (T_R) [N]	1.8±0.2	
Specific impulse (I_{spR}) [s]	43.0	
ON-delay [ms]	40	
OFF-delay [ms]	80	
Control cycle [ms]	200	
Control command cycle [ms]	10	
Arm1 [m]	0.3946	
Arm2 [m]	0.3104	

high and the thrusters are placed in the bottom of the vehicle, the thrusters only allows on/off commands, and the duration of the flight can only last up to 10 seconds in descending test.

2. FTB and System Setup

Figure 1 shows the image of FTB that is used in this paper. FTB has a CFRP tank with high pressure nitrogen to be used as the thrust for take off and landing. Specifications of the FTB are show in Table1. Compared to the usual rockets, the specific impulse is extremely low and the thrust forces of the thrusters are high enough for the take off.

The state equation of the FTB are as shown in equation (1) – (3). Although the testing time is very short, the FTB has low specific impulse, so the state equation of the mass is included. The forces in the equations are summation of the force produced by all of the thrusters for each direction.

$$\dot{\mathbf{x}} = \begin{pmatrix} \dot{X} \\ \dot{Y} \\ \dot{Z} \end{pmatrix} = \begin{pmatrix} u \cos \theta \cos \psi + v(\sin \phi \sin \theta \cos \psi - \cos \phi \cos \psi) \\ \quad + w(\cos \phi \sin \theta \cos \psi + \sin \phi \sin \psi) \\ u \cos \theta \sin \psi + v(\sin \phi \sin \theta \sin \psi + \cos \phi \cos \psi) \\ \quad + w(\cos \phi \sin \theta \sin \psi - \sin \phi \cos \psi) \\ -u \sin \theta + v \sin \phi \cos \theta + w \cos \phi \cos \theta \end{pmatrix} \quad (1)$$

$$m(\dot{u} + \omega_y w - \omega_z v) = -mg \sin \theta + F_x \quad (2)$$

$$m(\dot{v} + \omega_z u - \omega_x w) = mg \cos \theta \sin \phi + F_y \quad (2)$$

$$m(\dot{w} + \omega_x v - \omega_y u) = mg \cos \theta \cos \phi + F_z \quad (2)$$

$$\dot{m} = \frac{F_z}{I_{spM} g_E} + \frac{F_x + F_y}{I_{spR} g_E} \quad (3)$$

The forces in the state equations are given from the following equations. Equation (4) represents the horizontal forces driven by the roll (sub) thrusters. Equation (5) shows the vertical force produced by the main thrusters. These characteristics gives the FTB to have the ability with the limited force to

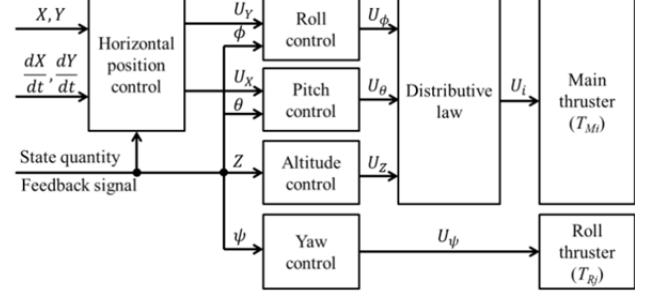


Fig.2 Flow chart of the control system.

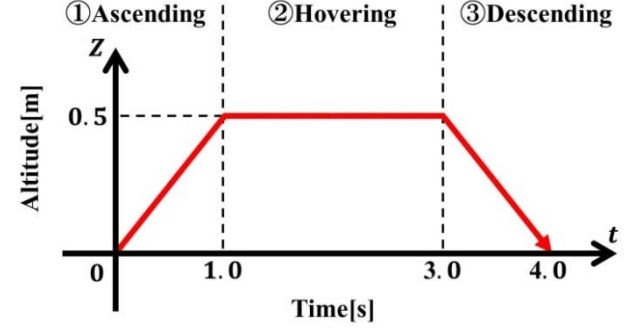


Fig.3 Example of testing scenario.

designated force in the desired direction, especially most of the force is produced in the vertical direction of the FTB. So the FTB has strong non-linearity to move in horizontal direction.

$$F_x = T_{R1} \cos \frac{\pi}{4} + T_{R4} \cos \frac{\pi}{4} - T_{R2} \cos \frac{\pi}{4} - T_{R3} \cos \frac{\pi}{4}$$

$$F_y = T_{R2} \sin \frac{\pi}{4} + T_{R3} \sin \frac{\pi}{4} - T_{R1} \sin \frac{\pi}{4} - T_{R4} \sin \frac{\pi}{4}$$

(4)

$$F_z = \sum_{i=1}^8 T_{Mi} \quad (5)$$

3. Control System

Figure 2 is the flow chart of the control system. Since the FTB cannot produce significant horizontal force, the horizontal position control comes before the altitude and attitude control. The horizontal position controller gives the desired attitude angle to move the FTB in the desired velocity / direction.

3.1. Altitude controller

First, the altitude controller is designed as follows. Equation (6) is the vertical controller for altitude control of the FTB.

$$U_z = M \left\{ 2\zeta_z \omega_z \left(\frac{dZ_r}{dt} - \frac{dZ}{dt} \right) + \omega_z^2 (Z_r - Z) + g_E \right\} - 4T_M \times 0.8 \quad (6)$$

The first group of the controller is simple PD controller to follow the desired velocity and altitude. The example of the designated values is shown in equation (7) and (8) and the

Fig.3 is the example scenario of the flight. As the first scenario, the FTB goes up, hovers and soft lands on the ground, thus the reference velocity is 0 throughout the test.

The gains are $\zeta_z = \sqrt{2}/2, \omega_z = \pi$.

$$Z_r = \begin{cases} 0.5t & (0.0 \leq t \leq 1.0) \\ 0.5 & (1.0 \leq t \leq 3.0) \\ -0.5t + 2.0 & (3.0 \leq t \leq 4.0) \\ 0 & (4.0 \leq t) \end{cases} \quad (7)$$

$$\frac{dZ_r}{dt} = 0 \quad (8)$$

The second group of the controller is the constant thrust given by the 4 even thrusters that are not used for the control. The constant value 0.8 is explained in section 3.4. The constant values of the thrust are subtracted from the required thrust.

3.2. Horizontal controller

The horizontal controller is designed as follows. The equations (9) and (10) show the horizontal controller. Similar to the altitude controller, the controller is simple PD controller to the designated position and velocity. The reference position and velocity, the position and the velocity are shown in equations (11) and (12). The gains are same as the ones used in the altitude controller.

$$U_x = M \left\{ 2\zeta_x \omega_x \left(\frac{dX_r}{dt} - \frac{dX}{dt} \right) + \omega_x^2 (X_r - X) \right\} \quad (9)$$

$$U_y = M \left\{ 2\zeta_y \omega_y \left(\frac{dY_r}{dt} - \frac{dY}{dt} \right) + \omega_y^2 (Y_r - Y) \right\} \quad (10)$$

$$X_r = Y_r = 0 \quad (11)$$

$$\frac{dX_r}{dt} = \frac{dY_r}{dt} = 0 \quad (12)$$

As the basic scenario for the initial testing, the reference position and velocity is set to 0, so the FTB tries to maintain the original position. As explained in the previous section, the FTB does not have ability to produce strong horizontal force, the input given as horizontal input is transformed into the reference attitude to move the FTB as show in equation (13) and (14)

$$\Delta X = \sin^{-1} \left(\frac{U_y}{4T_M \times 0.8} \right) \quad (13)$$

$$\Delta Y = -\sin^{-1} \left(\frac{U_x}{4T_M \times 0.8} \right) \quad (14)$$

3.3. Attitude controller

The attitude controller is designed as follows. Again, the equations (15), (16) and (17) show the attitude controller. The controller is simple PD controller to the designated angle and angular velocity. The reference angle for the roll and pitch angles are given from the desired attitude angle derived from equations (13) and (14). The desired angle for the yaw angle

is set to 0. The reference angular velocity during the flight are set as 0 as shown in equation (18). The gains are also same as the ones used in the altitude controller.

$$U_\phi = I_{xx} \left\{ 2\zeta_\phi \omega_\phi \left(\frac{d\phi_r}{dt} - \frac{d\phi}{dt} \right) + \omega_\phi^2 (\Delta X - \phi) \right\} \quad (15)$$

$$U_\theta = I_{yy} \left\{ 2\zeta_\theta \omega_\theta \left(\frac{d\theta_r}{dt} - \frac{d\theta}{dt} \right) + \omega_\theta^2 (\Delta Y - \theta) \right\} \quad (16)$$

$$U_\psi = I_{zz} \left\{ 2\zeta_\psi \omega_\psi \left(\frac{d\psi_r}{dt} - \frac{d\psi}{dt} \right) \right\} \quad (17)$$

$$\frac{d\phi_r}{dt} = \frac{d\theta_r}{dt} = \frac{d\psi_r}{dt} = 0 \quad (18)$$

3.4. Distributive law

In previous sections, the input force for each direction and angle are derived. In this section, the distributive laws for each thruster are explained. First, thrusters are distributed in set of 2 along the diagonal axis in x-y plane. Although there is small displacement, 2 thrusters have similar ability and displacement. The required force for the take off is close to 1000N which is similar to 70% of the thrust available. To control, the FTB properly, the odd numbered thrusters are chosen to have the constant command through out the flight as shown in Fig.4. Every cycle of the control is 200ms, and the ON command is given at 0ms of each cycle. The odd thrusters keep the ON command till 120ms of the cycle. Together with the ON delay and OFF delay that appears in the thrusters, the active time for the odd thrusters are 160ms during each cycle. So the odd thrusters give 80% of the thrust for the whole flight. The 0.8 in the equations (6), (13) and (14) is given by this strategy. So the odd thrusters keep approximately 60 to 80 % of the thrust required for hovering.

The other inputs that are driven by the controllers are distributed to even thrusters. The inputs derived by the altitude, horizontal and attitude controller are distributed to each even thruster by their position distribution as shown in equations (19) – (22).

$$U_2 = \frac{1}{4} \left(U_z + \frac{U_\phi}{arm1} - \frac{U_\theta}{arm2} \right) \quad (19)$$

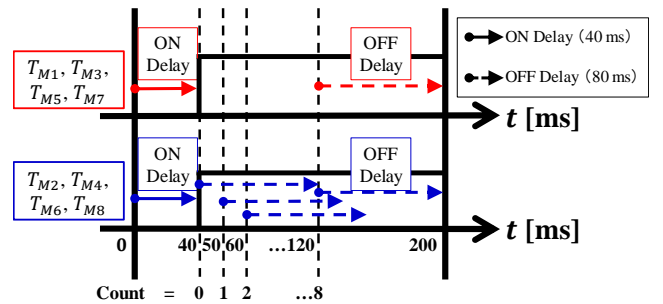


Fig.4 Thrust distribution count with time delay.

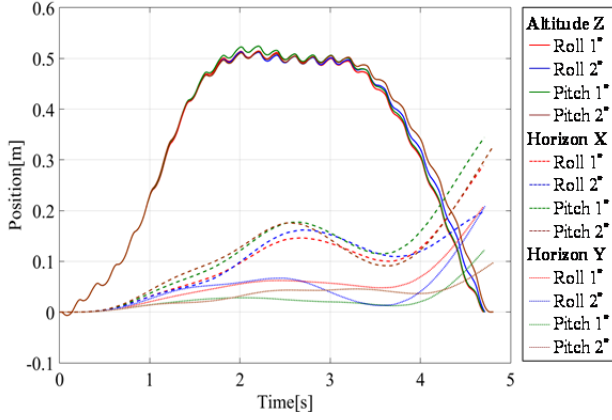


Fig.5 Flight trajectory of the original control law.

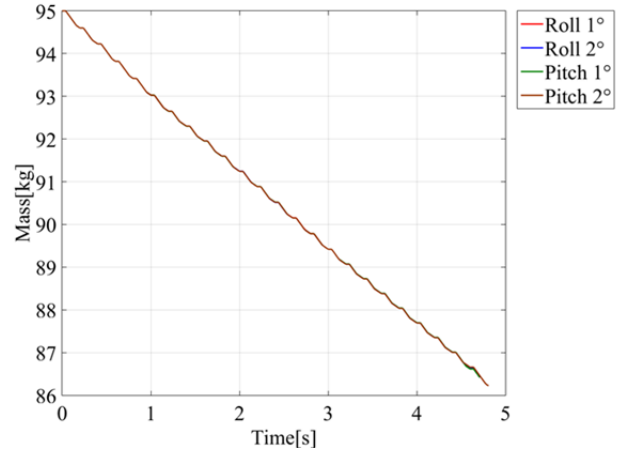


Fig.7 Time history of the fuel consumption of the original control law.

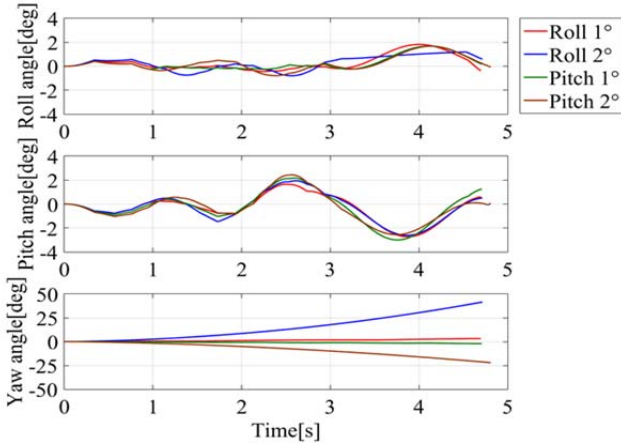


Fig.6 Attitude angle of the original control law.

$$U_4 = \frac{1}{4} \left(U_z + \frac{U_\phi}{arm2} + \frac{U_\theta}{arm1} \right) \quad (20)$$

$$U_6 = \frac{1}{4} \left(U_z - \frac{U_\phi}{arm1} + \frac{U_\theta}{arm2} \right) \quad (21)$$

$$U_8 = \frac{1}{4} \left(U_z - \frac{U_\phi}{arm2} - \frac{U_\theta}{arm1} \right) \quad (22)$$

After the input for each thruster is given, the values are now converted to the activation time according to the required thrust using equation (23). The thrusters have ability to command their valves every 10ms, so the inputs are transformed into OffCount with integer value of 0 to 8. The counts are applied to the count shown in Fig.4 to make the appropriate ON/OFF command for the control.

$$OffCount = \text{int} \left(\frac{U_i - 52}{8.6} \right) \quad (i = 2,4,6,8) \quad (23)$$

4. Simulation Results

The simulation results are shown in this chapter. The original controller explained in chapter 3 with some possible errors are shown first, the applied control to achieve better

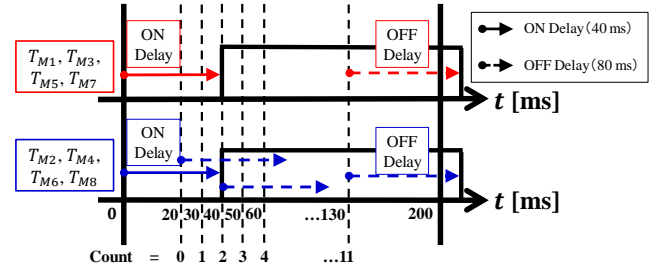


Fig.8 Thrust count algorithm for applied control law.

result follows. Possible scenario of flight test is shown in the last part of this chapter.

4.1. Original control law

In this section, the results by the original control law are explained. The FTB is expected to have some installation errors in the angle of the main thruster. They are expected to be 1 degree or so. Here, we have simulated the cases with the installation error in thruster 1 with 1 or 2 degree in roll and pitch angle. Figure 5 shows the trajectory of the flight with installation errors. The FTB flies with some vibrating motion with 5Hz, which is equal to the control frequency. The figure shows that the FTB moves in horizontal direction where the targets are 0.0m, but the maximum motion is within 0.5m, so they are not much of a problem. Figure 6 is the attitude angle during the flight. Roll and pitch angles keeps their values between 3 degrees. For the yaw angle, we can see that the value diverges as high as 45 degrees. This is due to the roll (sub) thrusters having very small value compared to the main thrusters. Only several degrees of miss displacement of the main thruster will cause the FTB to start spinning around. At this stage, the yaw attitude does not significantly cause any problem for the flight, but this problem should be solved before the future flight for long duration starts.

Figure 7 shows the time history of the fuel consumption during the flight. As seen from the graph, the value does not change much but decreases rapidly close to 2 kg/s this is one of the difficulties we face for this system.

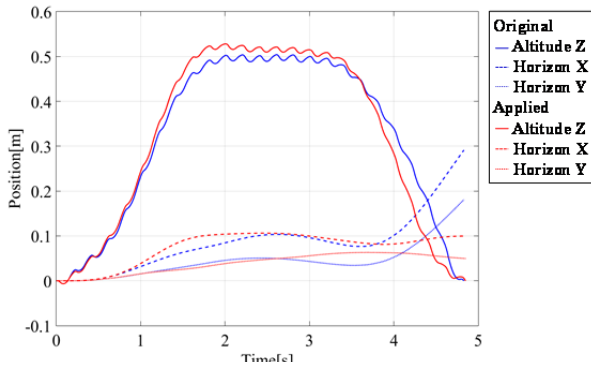


Fig.9 Comparison of flight trajectory.

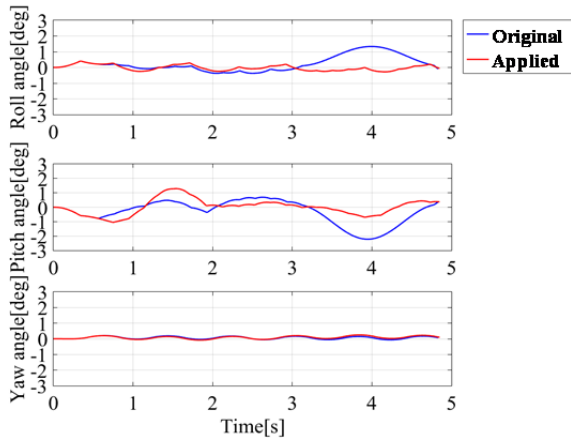


Fig.10 Comparison of the attitude angle.

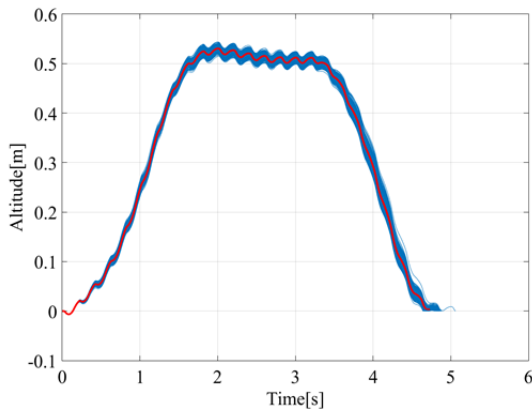


Fig.11 Monte Carlo simulation for applied control (altitude).

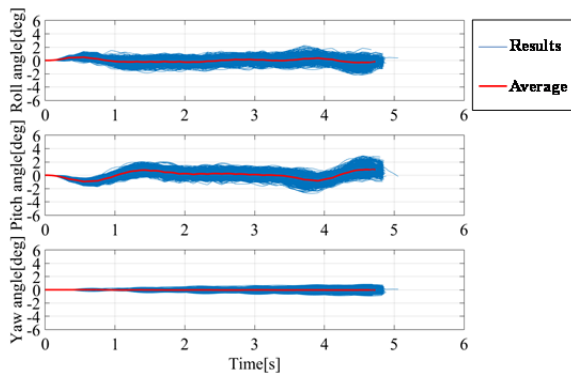


Fig.12 Monte Carlo simulation for applied control (attitude).

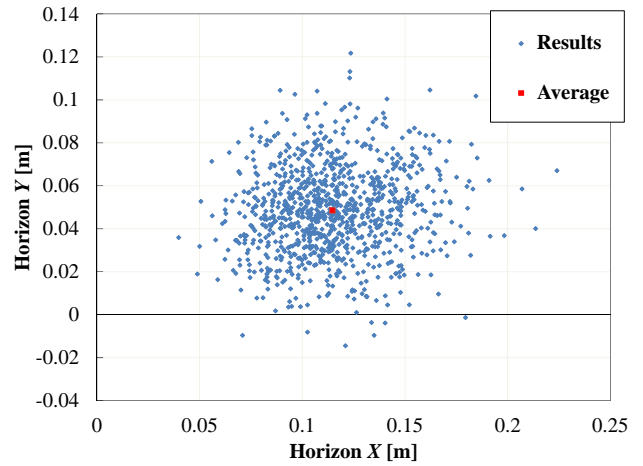


Fig.13 Monte Carlo simulation for applied control (altitude).

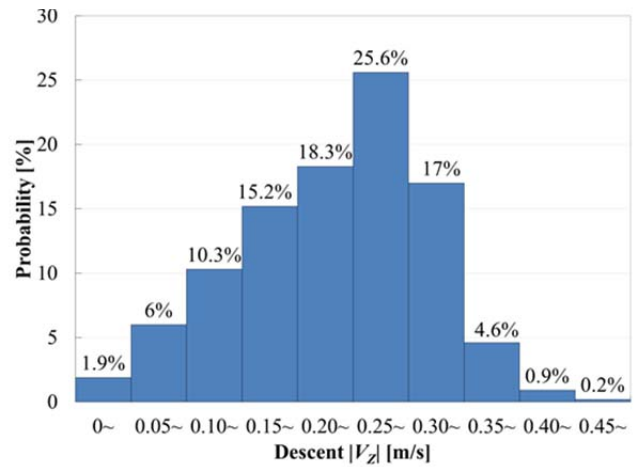


Fig.14 Monte Carlo simulation for applied control (terminal vertical velocity).

Although the original control law introduced in chapter 3 and section 4.1 has shown feasible flight ability, the control law is upgraded to achieve better flight. The thrust count algorithm is converted to the methodology shown in Fig.8. The count starts from the 20ms after the start and ends at 130 ms after the start. This will expand the ability of the control law to make the thrust to achieve 30% - 85% of the maximum thrust compared to 40% - 80% of the maximum thrust. Figures 9 and 10 shows the comparison of two control laws, where all other controllers other than the off count is the same. In every aspect, we can see that the applied control has better ability than the original control law.

Figure 11 - 14 shows the result of the Monte Carlo simulation of applied control law with deviation in the maximum thrust of main thrusters. The deviation is set as 3.5N where the main thrusters have possible deviation in there thrust. Altitude, attitude angle and terminal positions are basically within the range of the expected flight. Also, the terminal vertical velocity shown in Fig. 14 shows that most of the terminal velocities are under 0.3m/s where the maximum landing velocity for the soft landing is around 1.0m/s in current setup.

4.3. Descent simulation

In this section following the applied control law, another

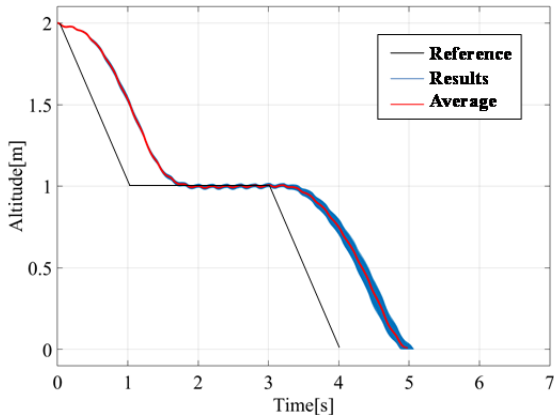


Fig.15 Monte Carlo simulation for descent test (altitude).

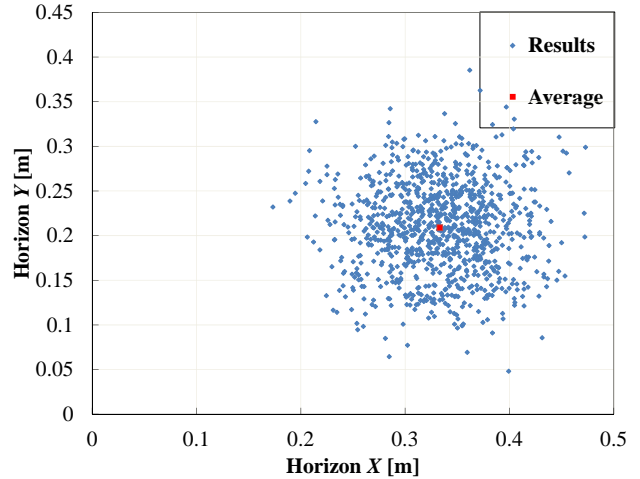


Fig.17 Monte Carlo simulation for descent test (altitude).

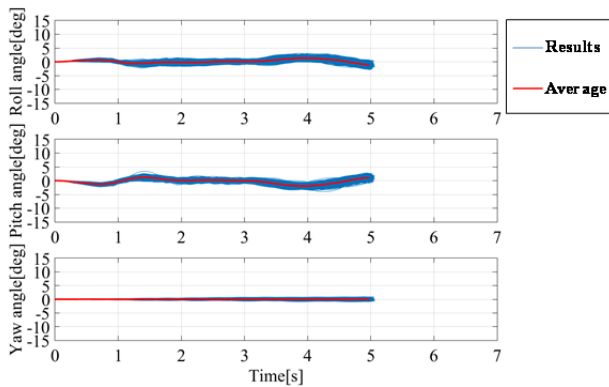


Fig.16 Monte Carlo simulation for descent test (attitude).

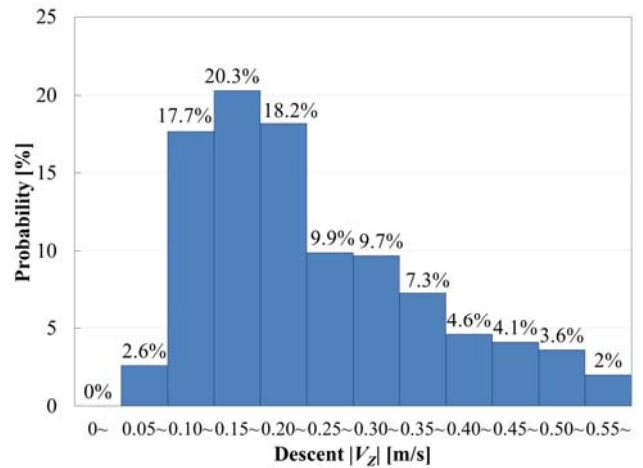


Fig.18 Monte Carlo simulation for descent test (terminal vertical velocity).

possible simulation for the FTB flight test is examined. The scenario is the descent test, where the FTB is dropped from the anchored condition and dropped. The flight reference is the solid black line shown in Fig.15. The results of the Monte Carlo simulation in the same conditions of the previous section has shown similar results with the last section, where all of the variables stays within the range of the expected flight. The higher terminal descent velocity in Fig.18 is caused by the steeper reference altitude given in the scenario, but the value itself is feasible for the soft landing.

5. Conclusions

In this paper, the flight control of FTB for future planetary landing is introduced and investigated with numerical simulations. Although there is difficulty of the FTB having short duration of flight, strong ON/OFF delays, small control frequency, and so on, the control system has shown feasible flight ability even with the errors that could appear for the actual flight. The control laws designed in this paper is expected to be loaded on the FY2017 FTB test held in May 2017.

References

- 1) Shin-ichiro Sakai et al., *Overview on a small lunar lander project*

- 1) *SLIM*, Proc of 60th Space Sciences and Technology Conference, 3C01(2016). (in Japanese)
- 2) Jon B. Olansen, Stephen R. Munday, Jennifer D. Mitchell, Michael Baine, *Morpheus: Advancing Technologies for Human Exploration*, Global Exploration Conference, GLEX-2012.05.2.4x12761(2012).
- 3) Timothy G. McGee et al., *Mighty Eagle: The Development and Flight Testing of an Autonomous Robotic Lander Test Bed*, Johns Hopkins Apl Technical Digest, Vol. 32, No. 3, 2013
- 4) NASA, *Masten's Xombie Flight Tests Astrobotic's Autonomous Landing System*, Space Technology Mission Directorate Flight Opportunities 2014 annual report, 47-53, 2014.
- 5) Tetujiro Ninomiya, et al., *Numerical simulations of the FTB test for lunar landing in the SELENE project*, NAL, ISSN 0389-4010 , 2001(in Japanese).
- 6) Yoshiro Hamada, et al., *A Study on the SELENE-B Model-Following Control System Using the Flying Test Bed*, Trans. of the JSME(C), 68(674), 2962-2969, 2002. (in Japanese)
- 7) Kazuhisa Fujita et al., *Preliminary Evaluation Test of a Flying Test Bed for Planetary Landing*, Proc. of JSME Annual Conference 2016, S1910201(2016). (in Japanese)
- 8) Toshiki Tamura, et al., *Study on Guidance and Control Law of a Flying Test Bed for Planetary Landing*, Proc. of Conf. on Automation Control, SaB4-2, pp.1311-1316, 2016.